Available online at www.sciencedirect.com
SCIENCE DIRECT®
Journal of the Mechanics and Physics of Solids
53 (2005) 1875–1891
JOURNAL OF THE MECHANICS AND PHYSICS OF SOLIDS
www.elsevier.com/locate/jmps

Actuation of the Kagome Double-Layer Grid. Part 2: Effect of imperfections on the measured and predicted actuation stiffness

D.D. Symons, J. Shieh[1], N.A. Fleck*

Engineering Department, Cambridge University, Trumpington Street, Cambridge, CB2 1PZ, UK

Received 27 August 2004; accepted 23 February 2005

Abstract

The actuation stiffness of a set of steel Kagome Double-Layer Grid (KDLG) structures with brazed joints is measured experimentally and compared with predictions by the finite element method. The predicted actuation stiffnesses for the perfect KDLGs much exceed the measured values, and it is argued that the low values of observed actuation stiffness are due to the presence of geometric imperfections introduced during manufacture. In order to assess the significance of geometric defects upon actuation stiffness, finite element calculations are performed on structures with a stochastic dispersion in nodal position from the perfectly periodic arrangement, and on structures with wavy bars. It is found that bar waviness has the dominant effect upon the actuation stiffness. The predicted actuation stiffness for the imperfect structures are in satisfactory agreement with the measured values assuming the same level of imperfection between theory and experiment.

Keywords: Elastic–plastic material; Structures; Finite elements; Mechanical testing; Morphing structures

*Corresponding author. Tel.: +44 1223332650; fax: +44 1223765046.
E-mail address: naf1@eng.cam.ac.uk (N.A. Fleck).
[1]Now at Department of Materials Science and Engineering, National Taiwan University, 1 Roosevelt Road, Sec. 4, Taipei, Taiwan.

0022-5096/$ - see front matter © 2005 Elsevier Ltd. All rights reserved.
doi:10.1016/j.jmps.2005.02.008

1. Introduction

There is much recent interest in the development of morphing materials that are stiff to external loads yet can accommodate large changes in shape upon actuation by lengthening (or shortening) a portion of the material. Hutchinson et al. (2003) have proposed that the planar Kagome truss is a suitable two-dimensional (2D) microstructure for shape changing (morphing) application. The finite planar Kagome truss, with suitable patch bars on the periphery is both statically and kinematically determinate in its pin-jointed form. Consequently, it is a rigid topology, but becomes a single-degree-of-freedom mechanism if any bar is replaced by an actuator. The Kagome topology has the additional advantage that the elastic, infinite planar Kagome truss is isotropic and has an in-plane modulus which attains the upper Hashin–Shtrikman bound, see Hyun and Torquato (2002). Practical morphing materials have, by necessity, rigid (welded) joints. Wicks and Guest (2004) have shown that the rigid joint 2D Kagome truss provides a low resistance to actuation compared to a fully triangulated planar grid.

The Kagome Double Layer Grid (KDLG) is a sandwich construction comprising two planar Kagome trusses and a double-layer tetrahedral core, see Fig. 1. The KDLG has been proposed by Hutchinson et al. (2003) and in Part I of this study (Symons et al., 2004) as a suitable microstructure for morphing plate structures. The plate extensional stiffness and plate bending stiffness of the KDLG are high due to the fact that it behaves as a sandwich plate with planar Kagome grids as the faces.

The infinite, periodic KDLG is neither statically nor kinematically determinate. However, Symons et al. (2004) have shown that the finite pin-jointed KDLG can be made to be statically and kinematically determinate by two modifications to its geometry. The structure is made asymmetric about its mid-plane (termed the asymmetric KDLG), and is given additional patch bars on its periphery, see Fig. 1. Consequently, the rigid jointed version of this *asymmetric patched KDLG* is a stiff, stretching dominated structure under passive external loading. Now consider the removal of any bar from the pin-jointed *asymmetric patched KDLG*; the structure behaves as a mechanism with a single degree of freedom. The rigid jointed version

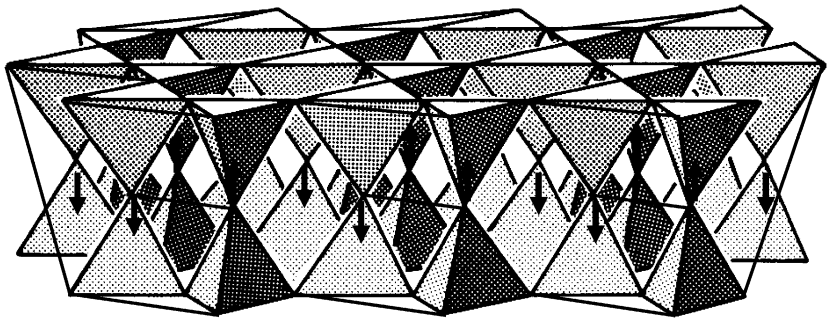

Fig. 1. Topology of Kagome Double Layer Grid (KDLG) showing asymmetric modification and patching schemes (the solid tetrahedra are representative only, in the real structure the faces are absent).

reflects this property: when one or more bars are elongated by suitable actuators, the rigid jointed structure resists this actuation by a compliant deformation mode dominated by bar bending. The deformation mode reduces to an internal collapse mechanism in the pin-jointed limit. Thus, the asymmetric patched KDLG is an attractive topology for a morphing structure.

1.1. Imperfection sensitivity

Practical, as-manufactured structures contain geometric imperfections. These imperfections may influence both the passive and active structural response, and it is the aim of the present study to investigate the sensitivity of the actuation stiffness of the KDLG to imperfections.

The effect of imperfections upon the macroscopic stiffness and strength of a lattice material is dependent upon both the type of imperfection and the mode of deformation exhibited by the perfect pin-jointed parent structure. For example, the fully triangulated 2D lattice (with a connectivity of six bars per joint) is a highly redundant stretching structure in pin-jointed form. An imperfection in the form of a random perturbation in the position of nodes has only a minor effect upon the overall stiffness and strength. In contrast, an imperfection in the form of waviness of each bar dramatically reduces the macroscopic stiffness and strength due to the large knock-down in axial stiffness and yield strength of each bar.

The regular hexagonal honeycomb has a different imperfection sensitivity to that of the fully triangulated structure. Under in-plane hydrostatic loading, the hexagonal honeycomb behaves as a stiff, stretching structure. However, on moving the nodes to form an irregular hexagonal honeycomb, hydrostatic loading causes the rigid jointed structure to deform in a much more compliant manner by the local bending of bars, see Chen et al. (1999, 2001). Similarly, the introduction of bar waviness degrades the structure from stretching-governed to bending-governed, for macroscopic hydrostatic loading, as reviewed by Chen et al. (1999). This behaviour is fundamentally different to that of the regular hexagonal honeycomb under in-plane deviatoric loading. Under deviatoric loading, the perfect structure deforms by bar bending, and the macroscopic stiffness and strength are relatively insensitive to the introduction of geometric defects, in the form of bar waviness and nodal position.

In Part I of this study, Symons et al. (2004) explored theoretically the actuation response of finite perfect KDLGs. Upon actuation, the structure deforms by a combination of bar bending and stretching, and for such structures the significance of imperfections has not been resolved. In this paper, the predicted sensitivity of actuation stiffness to a random repositioning of nodes and to the degree of bar waviness are compared with measurements of actuation stiffness on fabricated KDLGs.

2. Introduction to the 7-hexagon KDLG

Symons et al. (2004) have studied the effect of the number of repeating unit cells within a pin-jointed KDLG upon the total number of collapse mechanisms and

states of self-stress within the structure. They demonstrated that conversion of the infinite, periodic KDLG to a finite form requires the addition of peripheral patch bars in order to remove the collapse mechanisms associated with the reduced connectivity at the periphery. Their analysis of the static determinacy of the patched and unpatched finite structures revealed the existence of states of self-stress, unless the structure has a very limited number of unit cells (less than 7). For example, the symmetric–unpatched structure with 7 hexagons on each face contains a single state of self-stress, see Fig. 2a. Symons et al. (2004) showed that such states of self-stress can be removed by breaking the symmetry of the structure about the mid-plane to produce a so-called *asymmetric version* of the KDLG. The 7-hexagon asymmetric–unpatched version is sketched in Fig. 2b.

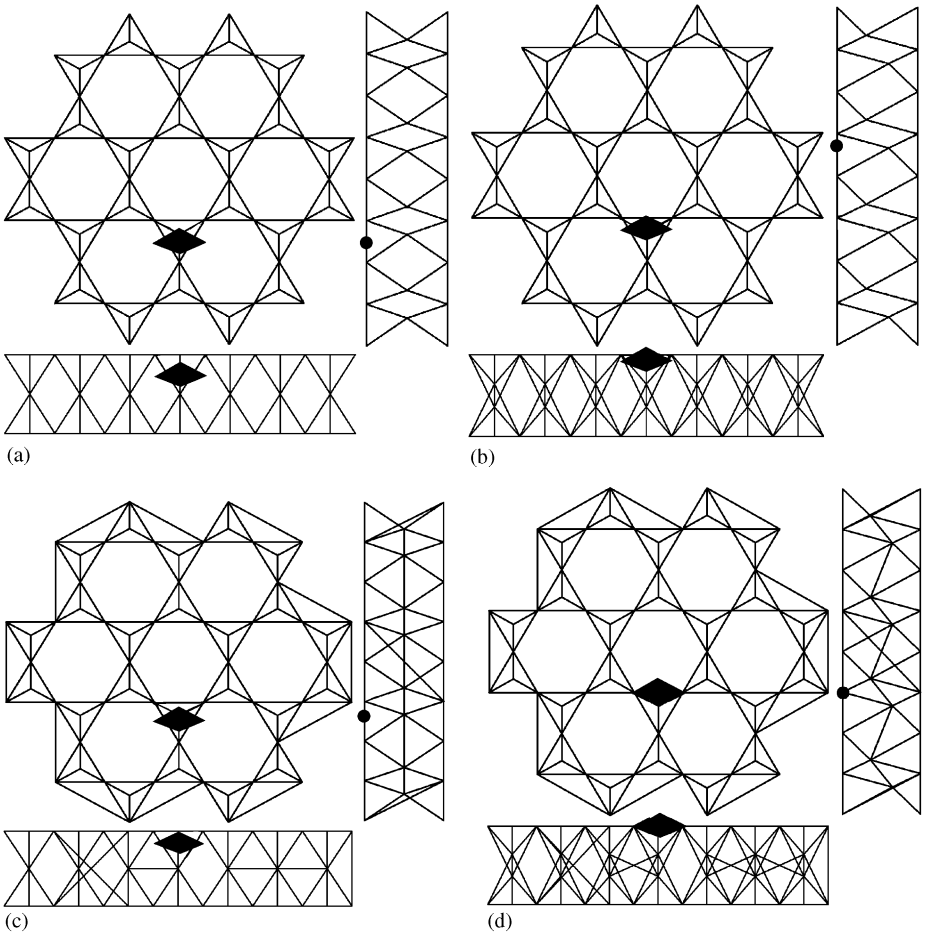

Fig. 2. Orthographic projections of four KDLG 7-hexagon variants: (a) symmetric–unpatched (S–U); (b) asymmetric–unpatched (A–U); (c) symmetric–patched (S–P); (d) asymmetric–patched (A–P).

In the present study, the actuation response of the 7-hexagon KDLG is measured and calculated for versions which are either symmetric (S) or asymmetric (A), and either patched (P) or unpatched (U). These four variants are labelled symmetric–unpatched (S–U), asymmetric–unpatched (A–U), symmetric–patched (S–P), and asymmetric–patched (A–P), and are catalogued in Fig. 2.

2.1. States of self-stress

The single state of self-stress in the pin-jointed S–U KDLG is triggered by the axial actuation of any bar associated with this state of self-stress. In contrast, the A–U KDLG, as shown in Fig. 2b, contains no states of self-stress, and provides no resistance when any bar is actuated. In rigid jointed form, a small resistance to actuation is anticipated due to bending of bars in the A–U grid, and a much larger resistance due to stretching of bars in the S–U grid.

2.2. Patching scheme

The A–U KDLG is statically determinate with no states of self-stress ($s = 0$), but it does contain $m = 30$ infinitesimal collapse mechanisms. To make the structure kinematically determinate ($m = 0$), yet remain statically determinate ($s = 0$), these 30 mechanisms are eliminated by a peripheral patching scheme, as shown in Fig. 2d. This patching scheme is applied to the top layer, mid-plane and bottom layer of the KDLG, with three additional bars.

Now consider the S–U KDLG. It contains a single state of self-stress ($s = 1$) and $m = 31$ mechanisms. The above patching scheme does not remove all mechanisms and the final count of states of self-stress and mechanisms for the symmetric–patched (S–P) grid is $s = 6$, $m = 6$ for the structure sketched in Fig. 2c. The number of mechanisms m and states of self-stress s for each of the above KDLG structures is summarised in Table 1.

2.3. Actuation of the KDLG

Symons et al. (2004) have explored theoretically the actuation response of the four variants of the 7-hexagon KDLG by replacing one bar with an axial actuator. They considered rigid-jointed structures and determined the sensitivity of actuation response to the *stockiness* S of the bars, as defined by the ratio of the radius of

Table 1
The four versions of the 7-hexagon KDLG

	Symmetric (S)	Asymmetric (A)
Unpatched (U)	S–U $s = 1$, $m = 31$	A–U $s = 0$, $m = 30$
Patched (P)	S–P $s = 6$, $m = 6$	A–P $s = 0$, $m = 0$

gyration λ to the length l of the bar,

$$S = \lambda/l. \tag{1}$$

The second moment of area I of the bar cross-section can be expressed by

$$I = A\lambda^2 \tag{2}$$

in terms of the cross-sectional area A and radius of gyration λ of the bar. Symons et al. (2004) showed that the achievable actuation strain is limited by the elastic buckling and yielding of the bars, and has a maximum value at a stockiness of $S = 0.004-0.1$, depending upon the assumed yield strain of the solid (ε_y in the range 0.1–1%).

3. Manufacture of KDLG structures

A single specimen of each of the four variants of 7-hexagon KDLG shown in Fig. 2 was manufactured by the assembly of two Kagome face sheets and two-folded tetrahedral core layers. The struts of the core and faces were laser cut from a low-carbon steel sheet using a CNC-controlled machine. The measured elastic–plastic uniaxial response of the steel sheet is given in Fig. 3a, measured at a strain rate of $10^{-3}\,s^{-1}$. The low-carbon steel has a measured Young's Modulus $E = 200$ GPa and a 0.2% offset yield strength of 200 MPa, giving a yield strain of 0.001. The constituent bars of the KDLGs were manufactured to a length of 40.5 mm, a square cross-section of 1×1 mm, and thereby a stockiness of $S = 0.007$. The previous study of Symons et al. (2004) shows that this value of stockiness is close to optimal for maximising the actuation strain, for the given value of yield strain. The two core component sheets were cold pressed by a CNC-controlled folding machine into their 3D form and were then assembled with the face sheets into the KDLG geometry. Two manual operations were used to bond together the structure: spot welding of the nodes, followed by reinforcement of the nodes by silver soldering with a gas flame and silver solder applied locally to each joint. Fig. 3b shows an example of a completed KDLG specimen: the S–U version.

The core geometry used in the construction of the asymmetric KDLG differs from that used for the symmetric KDLG, see Fig. 2. In the symmetric case, the nodes *on each face* of the folded tetrahedral core layers lie on the same plane, as in Figs. 2a and 2c. In the asymmetric case, the mid-plane nodes are perturbed in the through-thickness direction, as shown in Figs. 2b and 2d. The amplitude of the asymmetry of the nodes about the mid-plane of the asymmetric KDLG is equal to 14% of the total KDLG depth.

3.1. Measurement of imperfections in fabricated structures

A 3-axis co-ordinate measuring machine[2] was used to measure as-manufactured imperfections in the manufactured KDLG specimens. Imperfections in nodal

[2]An OMICRON A001 machine was used, with a sensor head tip radius of 0.5 mm.

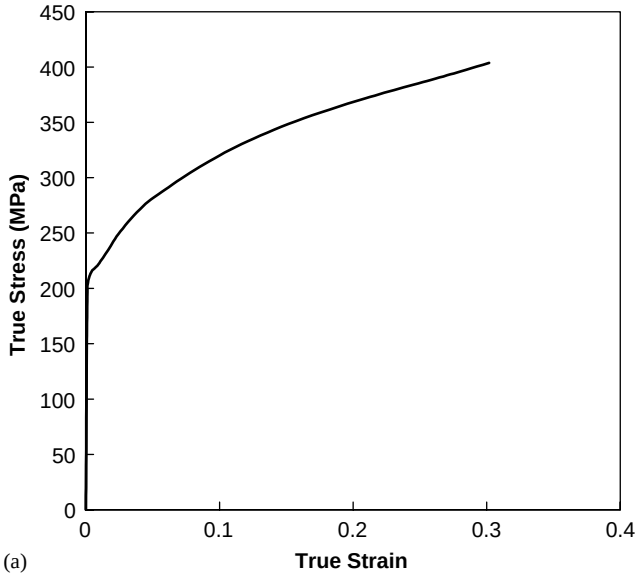

(a)

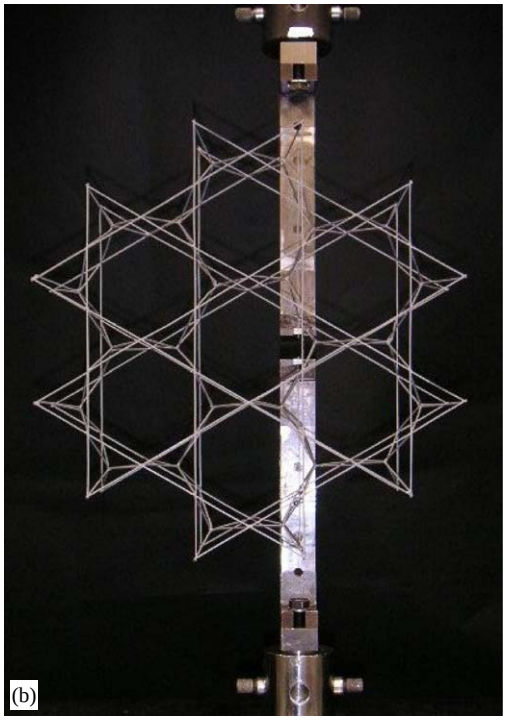

Fig. 3. (a) Uniaxial stress–strain curve of low-carbon steel; (b) 7-hexagon S–U KDLG specimen (bar length = 40.5 mm) and loading arrangement.

position were measured in both the through-thickness and in-plane directions. Additionally, the degree of bar waviness was measured by measuring the co-ordinates of each bar at mid-span in relation to its two ends. The degree of imperfection was measured for each variant of KDLG, and was found to show little variation from one type of structure to the next. Consequently, the values of imperfection reported below are averaged over measurements taken on all four variants.

The root mean square (RMS) value of nodal displacement in the through-thickness direction from that of the perfect structure was measured to be 2.1 mm. This imperfection is large relative to the bar cross-section of 1×1 mm, and is ascribed to the manual nature of the spot welding operation during specimen fabrication. The magnitude of the imperfection of nodal location in the plane of the KDLG is defined by the RMS value of the radial displacement of each node from that of the perfect lattice. This measured RMS value of 0.23 mm is much less than the out-of-plane value of 2.1 mm, and the difference is ascribed to the fact that the Kagome face sheets were accurately cut by the CNC laser cutting machine. Finally, the RMS value of the amplitude w_0 of bar waviness was measured to be 0.55 mm.

4. Actuation of the fabricated KDLG structures

4.1. Test protocol

Each of the four KDLG structures was actuated by replacing a single bar of the central hexagon on one of the Kagome face trusses by an instrumented axial actuator. A screw-driven mechanical test machine was used as the actuator: the two nodes of the removed member were stretched apart in a direction parallel to that of the removed bar, using a pair of L-shaped loading fixtures (see Fig. 3b). The load was measured using the load cell of the test machine while the displacement of the two loading nodes was measured continuously by a laser extensometer. Five load–unload cycles were applied to each specimen, incrementing the peak load in 10 N steps up to a maximum value of 50 N, at a displacement rate of 10^{-2} mm s^{-1}.

4.2. Measurements of actuation response

The actuation force versus deflection responses are plotted in Fig. 4a for the two symmetric KDLGs, and in Fig. 4b for the two asymmetric KDLGs. Finite element (FE) predictions of the loading response are included to allow comparison; details of the FE model are given later.

The initial measured stiffness of the structures decreases by a factor of 5 from most stiff to least stiff in the order S–P, S–U, A–P and A–U. The measurements confirm that symmetry and patch bars both contribute to the actuation stiffness. The symmetric patched (S–P) structure is essentially linear elastic over the applied load range (up to 50 N). However, the less stiff KDLGs show increasing hysteresis with

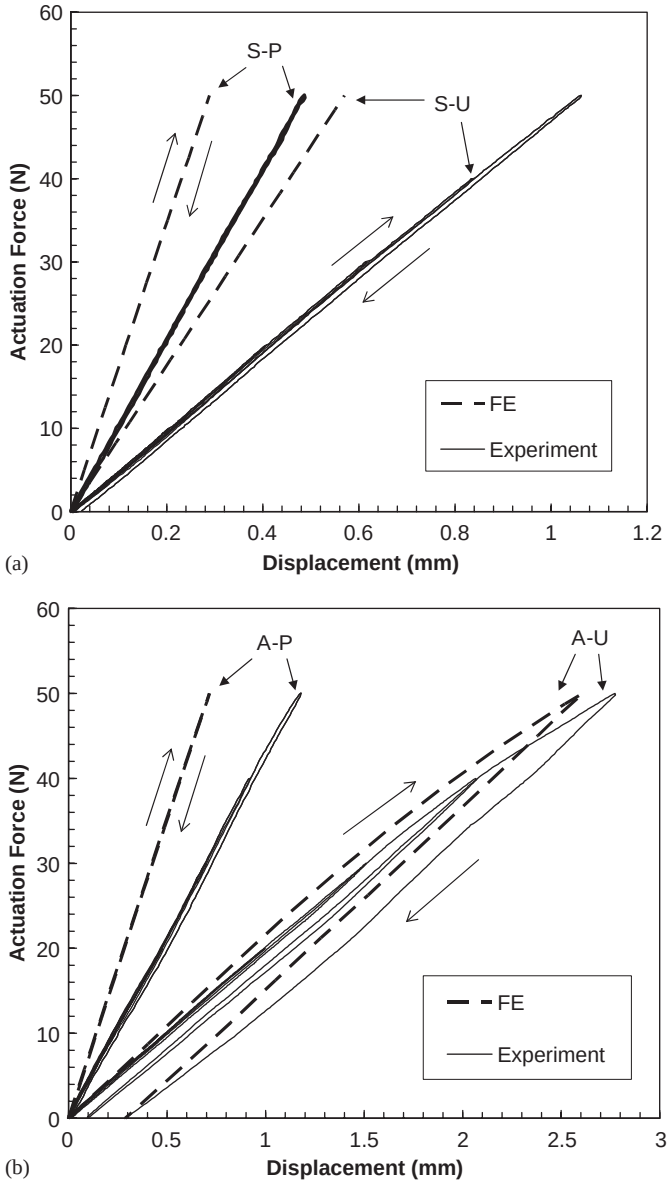

Fig. 4. Predicted and measured load versus displacement response of (a) symmetric, (b) asymmetric KDLG specimens. The finite element predictions, labelled FE, assume finite deformations and an elastic–plastic material response.

increasing load level in their force–deflection responses, due to plastic deformation within the struts. For example, when the asymmetric unpatched (A–U) structure was loaded up to 50 N (and 2.8 mm actuation) the residual deflection was 0.3 mm.

5. Predicted actuation response

Actuation of the KDLG structures by extension of the single central bar has been simulated by FE analysis. Recall that the position of the actuated bar in each 7-hexagon variant is shown in Fig. 2. The actuated bar is removed and pinned displacement constraints are applied so that the relative separation of the end nodes of the replaced bar is prescribed. The axial force between these two end nodes is calculated as a function of nodal separation. No rotational constraints are applied to any nodes other than those required to eliminate rigid body motion.

5.1. Prediction of actuation stiffness

Two commercially available FE packages were used to calculate the initial actuation stiffness of the structures: Pro/Mechanica (PTC, 2001) and ABAQUS/Standard (HKS, 2003). Both the Pro/Mechanica and ABAQUS simulations assumed linear elastic, infinitesimal displacements in order to calculate the initial actuation stiffness. The struts comprise an isotropic elastic solid of Young's modulus 200 GPa and Poisson ratio 0.3.

Pro/Mechanica uses a p-version of the FE method. Theoretical foundations of the p-method are given by Babuska et al. (1981) and Babuska and Szabo (1982). The basic idea is that the degree of interpolation function within each element can be adjusted to give any desired convergence accuracy. This method allows for automatic convergence by a multi-pass process: the element order is refined as required to give any desired solution accuracy, here taken to be 1% on actuation stiffness. The constituent bars of the KDLG were treated as single elements. Timoshenko (shear flexible) beams were employed with the joints treated as rigid nodes.

The element order in the ABAQUS program is controlled manually by the user. In the ABAQUS simulations, a single "B33" 2-node cubic beam element was used for each strut. The B33 element is an Euler–Bernoulli beam that does not allow for shear deformation. The actuation stiffnesses obtained by the two FE procedures are compared in Table 2. The differences between the Pro/Mechanica and ABAQUS results are sufficiently small for us to conclude:

(i) shear deformation is insignificant for these structures, and
(ii) the ABAQUS calculations, based on a single element per bar with cubic interpolation, suffice for our purposes.

5.2. Prediction of non-linear actuation response

The above calculations of actuation stiffness give no information on the effects of finite deformation and material non-linearity upon the response of the perfect structures. Leung et al. (2004) have shown that geometric softening occurs in actuated planar Kagome trusses due to finite deformation effects. It is clear from the

Table 2
Measured and predicted actuation stiffness of 7-hexagon KDLGs

	S–P	S–U	A–P	A–U
Pro/Mechanica (N/mm)	174.18	87.46	72.08	21.72
ABAQUS (N/mm)	174.21	87.48	72.17	21.75
% difference	0.019	0.022	0.12	0.17

Table 3
Comparison of measured and predicted initial actuation stiffness

	S–P	S–U	A–P	A–U
Measured (N/mm)	100	49	42	20
Prediction (N/mm)	174.2	87.5	72.2	21.8
Ratio	0.57	0.56	0.58	0.92

observed hysteresis in actuation response that significant plastic deformation occurs in the KDLG structures. In order to determine whether the observed actuation response can be captured by a full non-linear FE analysis of the perfect structure, additional ABAQUS predictions of actuation were made for the four KDLG variants, employing both geometric and material non-linearity.

The non-linear calculations were performed with 10 type B33 elements used to model each beam, in order to capture local non-linear effects. The measured elastic–plastic uniaxial response of the steel sheet was employed, recall Fig. 3a, with von Mises plastic flow theory and isotropic hardening. The FE predictions of the loading and unloading actuation force versus displacement for the four perfect variants, loaded up to 50 N, are included in Figs. 4a and 4b. The predictions for the symmetric (S–P and S–U) and the asymmetric–patched (A–P) structures give the same linear response as that obtained by the previous linear FE analyses as summarised in Table 2. In contrast, the asymmetric–unpatched (A–U) KDLG gives pronounced non-linearity at loads exceeding 30 N. The hysteresis present in the predicted response of the A–U structure is due to material non-linearity, and the linear unloading response indicated that finite deformation effects can be ignored.

5.3. Comparison of predicted actuation stiffness for perfect geometry with measured response

The measured initial stiffnesses are compared with FE predictions in Table 3 and in Fig. 4. Only in the case of the asymmetric–unpatched (A–U) KDLG does the measured experimental actuation stiffness show good agreement with the FE prediction. The measured stiffness of the other three structures is significantly lower than the prediction.

6. Predicted sensitivity to manufacturing imperfections

It has already been noted that the manufacturing method gives rise to geometric imperfections in the form of misplaced nodes and bar waviness. We proceed to predict the sensitivity of actuation stiffness to each type of imperfection, and then to compare the predicted actuation stiffnesses of the as-manufactured grids with the observed values.

6.1. Sensitivity of actuation stiffness to misplaced nodes

Recall from Section 3.1 that the RMS value of nodal perturbation, in the direction normal to the plane of the KDLG, equals 2.1 mm. The magnitude of the imperfection of nodal location within the plane of the KDLG has already been defined by the RMS value of radial displacement of each node from that of the perfect lattice; the measured RMS value for in-plane perturbation equals 0.23 mm. The FE method using the ABAQUS package is now used to predict first the effect of through-thickness nodal imperfection, and second the effect of in-plane nodal imperfection upon actuation stiffness.

A MATLAB (Mathworks, 2002) routine is used to displace randomly every node in the ABAQUS input file from that of the perfect structure, for any chosen amplitude of imperfection. The FE model uses only a single beam element for each bar and so the bars remain straight after movement of the structural nodes. Ten structural realisations were constructed by the MATLAB routine for any given amplitude of imperfection in order to gauge the dispersion in actuation stiffness from one realisation to the next. The 10 calculations were then used to deduce the mean and standard deviation.[3]

Fig. 5a shows a plot of the mean and 95% confidence limits (± 2 standard deviations) of the actuation stiffness for the four 7-hexagon KDLGS versus the magnitude of nodal movement in the through-thickness direction. Likewise, Fig. 5b shows a plot of the mean and 95% confidence limits of the actuation stiffness of the four KDLGS with increasing in-plane imperfection. In both plots, the RMS value of nodal imperfection has been normalised by the bar length ($l = 40.5$ mm).

Take the two figures together, and consider first the mean values of the responses. Out-of-plane and in-plane imperfections have only a minor effect upon the actuation stiffness for the asymmetric KDLGs, but lead to a significant drop in actuation stiffness for the symmetric KDLGs. Recall that the pin-jointed symmetric structures contain a number of internal states of self-stress which are activated by bar actuation. Geometric imperfections break the symmetry of the structure and remove these states of self-stress in the pin-jointed version. Consequently, the actuation stiffness of the rigid-jointed symmetric grids are reduced.

It is further noted from Figs. 5a and b that the predicted actuation stiffness displays significant scatter from one structural realisation to the next: the spread in

[3]It would be preferable to perform additional simulations to give statistically significant results, but this was prohibitively time consuming.

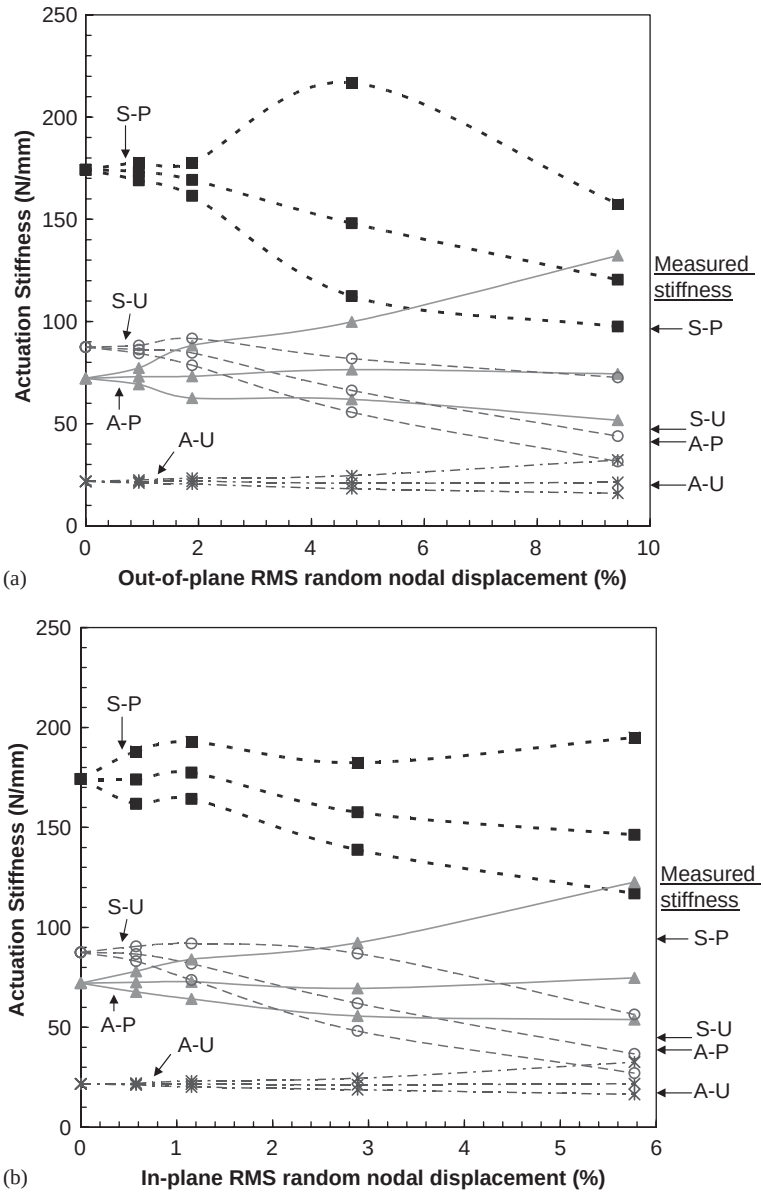

Fig. 5. Actuation stiffness of KDLGs with (a) out-of-plane, (b) in-plane nodal imperfection (mean and 95% confidence limits). The measured actuation stiffness is given on the right-hand side for comparison.

the 95% confidence limits increases with overall magnitude of imperfection for all topologies, with the largest dispersion evident for the patched structures. Such scatter is of practical concern and suggests the need for tight quality control in manufacture.

6.2. Effect of bar waviness upon actuation stiffness

Waviness of a bar leads to a reduction in its axial stiffness but to a negligible change of its bending stiffness. Consider a bar with pre-existing sinusoidal waviness of amplitude w_0 and wavelength l'. Assume that the bar length l spans an integral number of semi-wavelengths of waviness, such that $nl' = 2l$, where n is a positive integer. Then, the axial stiffness k of the bar is reduced by the factor $1 + \frac{1}{2}e^2$ in terms of the waviness normalised by the radius of gyration, $e \equiv \sim w_0/\lambda$. This knock-down in stiffness can be large. For example, consider a bar of 1 mm square cross-section, and waviness of amplitude 0.6 mm. Then, e equals 2.1 and the axial stiffness of the bar is reduced from $k = EA/l$ to $k = 0.31EA/l$, where as before E denotes Young's modulus and A the cross-sectional area of the bar.

It is straightforward to model the effect of bar waviness upon the bar properties within a FE model. Recall that the effect of bar waviness is to reduce the effective axial stiffness of a bar while leaving its bending stiffness unchanged. This can be achieved by reducing the cross-sectional area of the bar by the factor $(1 + e^2/2)$, while leaving the bending modulus EI unchanged. FE calculations of this type have been performed using the ABAQUS program: all bars in the KDLG are ascribed the same level of waviness, and the actuation stiffness is determined as a function of e for each of the four variants shown in Fig. 2. It is emphasised that the nodal positions are those of the perfect structure.

Fig. 6 contains a plot of the actuation stiffness of the four KDLG variants as a function of the non-dimensional bar waviness imperfection e. The A–U KDLG is bending dominated in its performance and is largely unaffected by bar waviness. In contrast, the S–P KDLG is stretching dominated and shows a large drop in actuation stiffness with increasing bar waviness. The A–P and S–U cases are intermediate.

6.3. Comparison of predicted and measured actuation stiffness for imperfect KDLGs

It remains to match the predicted actuation stiffness for the imperfect structures and the observed actuation stiffness for the four KDLGs. Recall from Table 3 that all KDLGs except for the A–U variant have an observed actuation stiffness of 56–58% that of the perfect structure. It is clear from Figs. 5a and 5b that imperfections in nodal position (both out-of-plane and in-plane) lead to only a small drop in mean value of actuation stiffness for the symmetric KDLGs and to a negligible change for the asymmetric KDLGs. The confidence limits in Figs. 5a and 5b reveal that nodal imperfections of the magnitude observed could not give rise to the knock-down observed for three of the structures. In contrast, bar waviness is a promising candidate for the source of the reduction in actuation stiffness: it is clear from Fig. 6 that bar waviness leads to a drop in stiffness for the same three variants as that noted in Table 3. But is there quantitative agreement between predicted and measured actuation stiffness for the imperfect structures?

The predicted actuation stiffness is plotted against the measured stiffness for selected amplitudes of bar waviness in Fig. 7. It is seen that a non-dimensional

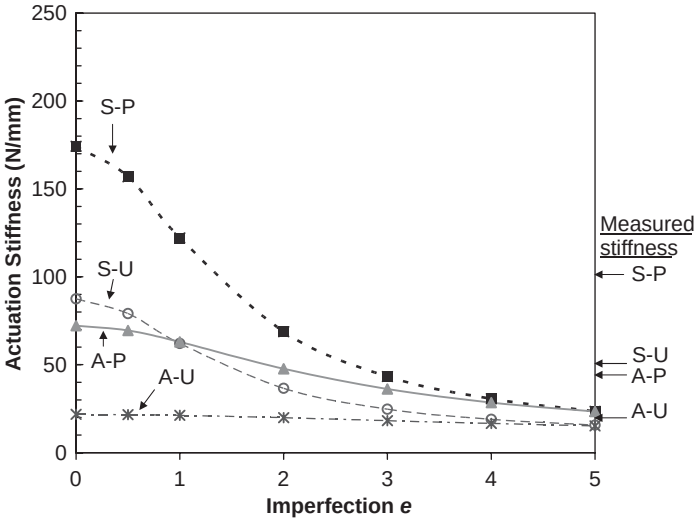

Fig. 6. Effect of bar waviness on actuation stiffness.

amplitude of $e = 1.5$ ($w_0 = 0.43$ mm) provides reasonable agreement for all four variants of KDLG. This magnitude of waviness is in satisfactory agreement with the measured value of $e = 2.0$ ($w_0 = 0.55$ mm). It is concluded that the measured values of actuation stiffness can be explained in terms of as-manufactured bar waviness.

7. Concluding remarks

In this study, the sensitivity of the actuation performance of the Kagome Double-Layer Grid (KDLG) to manufacturing defects is explored. The FE simulations demonstrate that the observed knock-down in actuation stiffness due to imperfections is a consequence of bar waviness rather than the misplacement of nodes. It is also shown that the actuation stiffness of both the perfect and imperfect grids depend upon the detailed topology of the grids—whether symmetric or asymmetric, and whether patched or unpatched.

Insight into the differences in actuation stiffness from one variant of KDLG to the next is achieved by examining the pin-jointed parent structures. First, consider the symmetric–patched pin-jointed KDLG. In the absence of imperfections, it contains six states of self-stress, as detailed in Table 1. The extension of a bar by actuation triggers one or more of these states of self-stress, and the remaining structure resists actuation by the storage of elastic energy by bar stretching (and bending). The introduction of bar waviness leads to a sharp drop in the axial stiffness of the bars, and thereby to a drop in actuation stiffness, see Fig. 6. Alternatively, an imperfection in the form of a random movement of nodes removes the states of self-stress in the

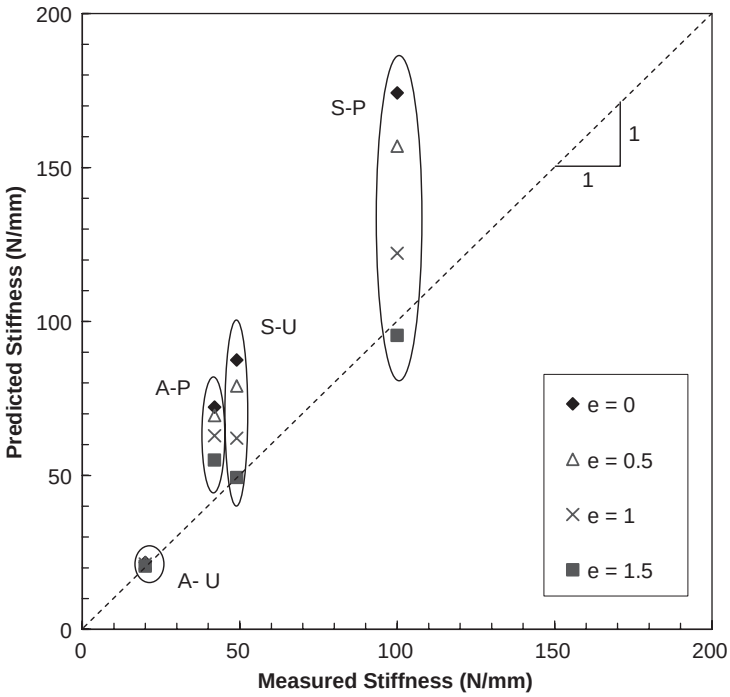

Fig. 7. Measured actuation stiffness of KDLG specimens plotted against predicted stiffness for bar waviness imperfection $e = 0$, 0.5, 1 and 1.5.

pin-jointed structure, and this is reflected by a reduction in actuation stiffness of the rigid-jointed version, recall Figs. 5a and b.

Second, consider the asymmetric–patched KDLG. In its pin-jointed form, with one bar removed, the patched structure A–P contains a single mechanism, and can be actuated freely, with zero resistance by the surrounding structure. Random movement of nodes changes neither the number of states of self-stress (zero) nor the number of mechanisms (one), and consequently the rigid-jointed version has a negligible change in mean actuation stiffness with increasing nodal imperfection, see Figs. 5a and b. The moderate actuation stiffness of the rigid-jointed perfect version is due to the moderate level of stockiness of bars considered in this investigation. Consequently, the structure has some stretching resistance, and this is reduced by the introduction of bar waviness, see Fig. 6.

Finally, consider the asymmetric–unpatched (A–U) KDLG. The perfect, pin-jointed version with one bar removed has no states of self-stress but does possess 30 mechanisms. The random movement of nodes has no effect upon the number of states of self-stress and mechanisms, and consequently the actuation stiffness of the rigid-jointed version is insensitive to the repositioning of nodes, recall Figs. 5a and b. The rigid-jointed A–U KDLG deforms predominantly by bending of its constituent

bars. Since the bending stiffness of a bar is almost insensitive to the presence of bar waviness, the actuation stiffness is almost independent of bar waviness, as shown in Fig. 6. The actuation stiffnesses of the perfect and imperfect A–U grid are least of all the KDLG grids investigated, due to the fact that the structure is bending dominated.

Acknowledgements

The authors are grateful for financial support from a DARPA grant on synthetic multi-functional materials and wish to thank Profs. A. G. Evans and J. W. Hutchinson for helpful discussions.

References

Babuska, I., Szabo, B.A., 1982. On the rates of convergence of the finite element method. Int. J. Numer. Methods Eng. 18, 323–341.

Babuska, I., Szabo, B.A., Katz, I.N., 1981. The p-version of the finite element method. SIAM J. Numer. Anal. 18, 515–545.

Chen, C., Lu, T.J., Fleck, N.A., 1999. Effect of imperfections on the yielding of two-dimensional foams. J. Mech. Phys. Solids 47, 2235–2272.

Chen, C., Lu, T.J., Fleck, N.A., 2001. Effect of inclusions and holes on the stiffness and strength of honeycombs. Int. J. Mech. Sci. 43, 487–504.

HKS, 2003. ABAQUS/Standard Version 6.3.1. Hibbit, Karlsson and Sorenson Inc., Providence, RI.

Hutchinson, R.G., Wicks, N., Evans, A.G., Fleck, N.A., Hutchinson, J.W., 2003. Kagome plate structures for actuation. Int. J. Solids Struct. 40, 6969–6980.

Hyun, S., Torquato, S., 2002. Optimal and manufacturable two-dimensional, Kagomé-like cellular solids. J. Mater. Res. 7, 137.

Leung, A.C.H., Symons D.D., Guest, S.D., 2004. Actuation of Kagome lattice structures. 45th AIAA/ASME/ASCE/AHS/ASC Structures, Structural Dynamics and Materials Conference, Palm Springs, CA, 19–22 April 2004.

MathWorks, 2002. MATLAB Version 6.5. The MathWorks Inc., 3 Apple Hill Drive, Natick, MA 01760-2098, USA.

PTC, 2001. Pro/MECHANICA Version 23.3. Parametric Technology Corporation, Needham, MA.

Symons, D.D., Hutchinson, R.G., Fleck, N.A., 2004. Actuation of the Kagome Double Layer Grid. Part I: prediction of performance of the perfect structure. J. Mech. Phys. Solids, to appear, doi:10.1016/j.jmps.2005.02.011.

Wicks, N., Guest, S.D., 2004. Single member actuation in large repetitive truss structures. Int. J. Solids Struct. 41, 965–978.